

An Improved Digital Watermarking Scheme for Image Copyright Protection using Morphological Skeleton and Wavelet Packets

Dragoş N. Vizireanu¹, Radu O. Preda²

Abstract – In this paper we propose a robust blind private watermarking algorithm for image Copyright protection. The algorithm is based on Wavelet Packets. Our basic idea is to decompose the original image into a series of details at different scales by using Wavelet Packets; the skeleton of a binary image, used as the watermark, is then embedded into the different levels of detail. Experiments showed that our algorithm does only minimal degradation to the original image and can improve the robustness of watermarking against different attacks.

Keywords – Blind, private Watermarking, Wavelet Packets, Morphological skeleton.

I. INTRODUCTION

Digital watermarking algorithms can generally be grouped into two main categories: those performed in the spatial domain and those in the frequency domain. Early techniques embedded the watermark in the least significant bits (LSBs) of image pixels [1]. However this technique and some other proposed improvements [2], [3] have relative low-bit capacity and are not resistant enough to lossy image compression, cropping and other image processing attacks. On the contrary frequency-domain-based techniques are more robust to attacks.

Procedures that can recover the hidden mark without the use of the original unmarked data are defined as *blind* decoding. Some of these blind techniques require access to a reference key to extract the mark. These are called *private*. Others, on the other hand, don't require the unmarked data either, nor do they need a key for decoding purposes. They are called public because everyone is allowed to access the watermarked data. From now on, the term DWT-based blind private watermarking technique should be meaningful.

The paper is organized as follows. In section II the Wavelet packets, a particular kind of wavelet decomposition that separates signals in symmetrical levels of detail is shortly described. Section III describes the mathematical morphology method used on the binary watermark image. Section IV presents the embedding and extraction strategies used by the proposed technique. Finally experimental results and conclusions are given in section V.

II. WAVELET ANALYSIS

The Discrete Wavelet Transform (DWT) is a special case of a subband transform, with a filter bank being the basic building block. The elements of the filter bank are a decomposition filter, a reconstruction filter, a downsampler and an upsampler. A multirate filter bank is a set of M parallel filters having either the same input or output. When the filters are used to split a common input x, it is referred to as an analysis filter bank. On the other hand, it is called a synthesis bank when it is used to form one common output.

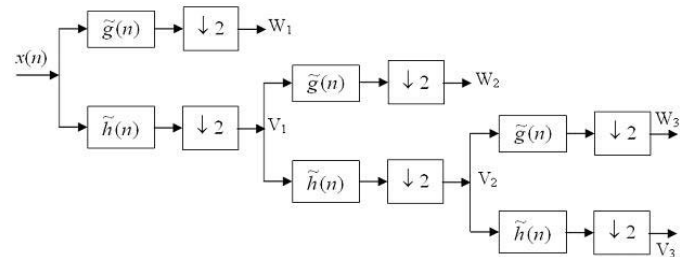


Fig. 1. Three level Wavelet decomposition

An important feature of multirate filter banks is that they split a signal into different frequency bands. Perfect reconstruction from the composition is maintained as long as specific filter requirements are fulfilled. Fig. 1 shows three levels of Wavelet decomposition using filter bank representation.

The multiresolution decomposition is described in terms of subspaces V_j and W_j , which relate to the intermediate signals at the output of the level j filter bank. As the number of decomposition levels used increases, the subspace number j increases as well.

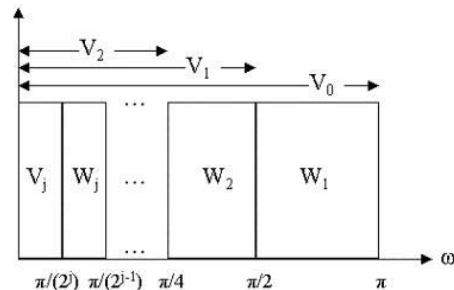


Fig. 2. Spectrum division after Wavelet decomposition

¹Dragoş N. Vizireanu is with the Electronics and Telecommunications Faculty, Bd. Iuliu Maniu Nr. 1-3, 061071 Bucharest, Romania, E-mail: nae@comm.pub.ro

²Radu O. Preda is with the Electronics and Telecommunications Faculty, Bd. Iuliu Maniu Nr. 1-3, 061071 Bucharest, Romania, E-mail: radu@comm.pub.ro

The Wavelet space W_j corresponds to the difference between the present scaling space V_j and previous one V_{j-1} . It means that $V_j \oplus W_j = V_{j-1}$ (see Fig. 2). The resulting decomposition bands are not of the same size, so we will try a different approach.

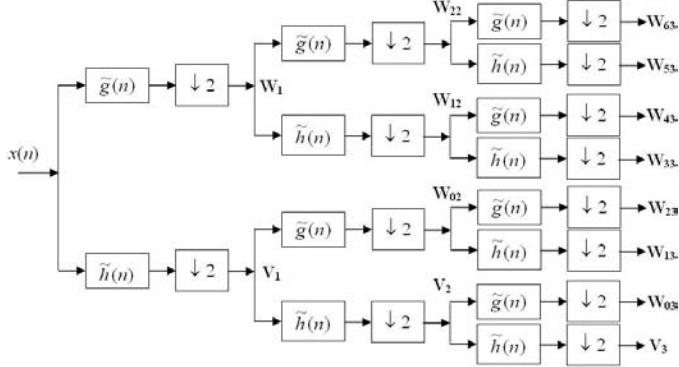


Fig. 3. Two level Wavelet Packets decomposition

One advantage of Wavelet Packets, important for our application, is the symmetry of the final decomposition bands. It means that all the bands are of the same size, and that the translation from frequency to time domain is much more straight-forward (see Fig. 4).

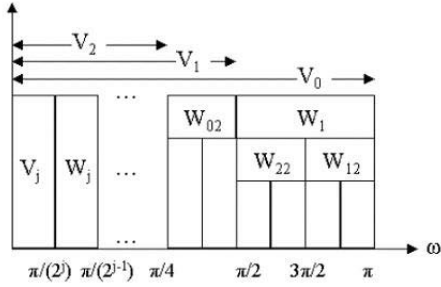


Fig. 4. Spectrum division after Wavelet Packet decomposition

III. MORPHOLOGICAL SKELETON

The skeleton is one of the main operators in mathematical morphology and it can be calculated entirely using the basic morphological operators.

Dilation and erosion are the fundamental operators of the Mathematical Morphology. The key process in the dilation and erosion operators is the local comparison of a shape, called structuring element, with the object to be transformed.

The structuring element is a predefined shape, which is used for morphological processing of the images. The most common shapes used as structuring elements are horizontal and vertical lines, squares, digital discs, crosses, etc.

The fundamental morphological operators are based on the operation of translation. Let B be a set contained in the Euclidean space E , and let x be a point in E . The translation of the set B by the point x , denoted B_x , is defined as follows:

$$B_x = \{b + x \mid b \in B\} \quad (1)$$

The dilation of the image X by the structuring element B , denoted $X \oplus B$, is defined by:

$$X \oplus B = \bigcup_{x \in X} B_x \quad (2)$$

For dilation: when the structuring element is positioned at a given point and it touches the object, then this point will appear in the result of the transformation, otherwise not.

The erosion of X by the structuring element B , denoted $X \ominus B$, is defined in the following way:

$$X \ominus B = \bigcap_{b \in B} X_{-b} \quad (3)$$

For erosion: when positioned at a given point, if the structuring element is included in the object, then this point will appear in the result of the transformation, otherwise not.

Based on the fundamental operators, two morphological operators are developed. These are the opening and closing operators. They are dual operators.

The opening operator, denoted “ \circ ”, can be expressed as a composition of erosion followed by dilation, both by the same input structuring element:

$$X \circ B = (X \ominus B) \oplus B \quad (4)$$

The closing operator, denoted “ \bullet ”, can be expressed as composition of dilation followed by erosion by the same input structuring element:

$$X \bullet B = (X \oplus B) \ominus B \quad (5)$$

Lantuejoul proved that the skeleton $S(X)$ of a topologically open shape X in Z^2 can be calculated by means of binary morphological operations, in the following way:

$$S(X) = \bigcup_{n>0} S_n(X) = \bigcup_{n>0} \{X \ominus nB - (X \ominus nB) \circ B\} \quad (6)$$

where B is a structuring element.

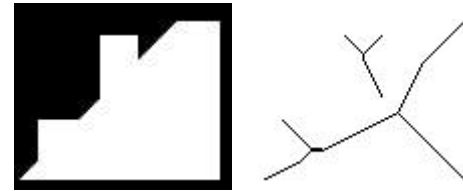


Fig. 5. The original image and its skeleton

In Fig. 5 a binary image and its morphological skeleton are shown. The skeleton is obtained using a cross as structuring element.

The compression rate for this example is about 4%. This means that, for the skeleton, we need 25 times less information in order to reconstruct the original image.

The reconstruction process needs additional information about the size of the structuring element for each point of the

skeleton. By adding the information about the structuring element to the skeleton, the resulting image can be considered as a greyscale image. In this case, the resulting image is shown in Fig. 6.



Fig. 6. The skeleton completed with structuring element information

The biggest problem with the skeleton representation is the fact that it contains many redundant points. These points are not needed for reconstruction, but appear in the skeleton.

The image representations obtained from these methods are called reduced skeletons: RS .

From the collection of subsets $\{S_n(X)\}_{n>0}$ and knowing the radius n for each pixel, the original shape X can be perfectly reconstructed in the following way:

$$X = \bigcup_{n \geq 0} S_n(X) \oplus nB \quad (7)$$

The Morphological Skeleton representation permits also partial reconstruction, yielding simplified versions of the original shape. This is obtained by eliminating from the skeleton the pixels with values smaller and equal to a given value k :

$$X \circ kB = \bigcup_{n \geq k} S_n(X) \oplus nB \quad (8)$$

The same results are obtained from the use of the reduced skeleton:

$$X = \bigcup_{n \geq 0} RS_n(X) \oplus nB \quad (9)$$

IV. THE WAVELET PACKETS BASED WATERMARKING SCHEME

Our goal is to hide the Copyright information in the original image using the Wavelet Packets' domain for the watermark embedding. The author uses a unique (secret) binary identification key of 128 bits to allow the recovery of the mark. The main steps of our embedding technique are presented in the following.

a) First the owner's identification key of 128 bits is randomly generated. 128 bits are enough to grant uniqueness of the key and protect the owner. This key is stored and kept secret.

b) The first 8 bits in the secret key are used to select the wavelet decomposition scheme (the Wavelet functions used and the number of decomposition levels). The multitude of basis functions available increases the security of our scheme.

The Wavelet families used are Coiflets, Daubechies and biorthogonal and the maximum level of decomposition is L .

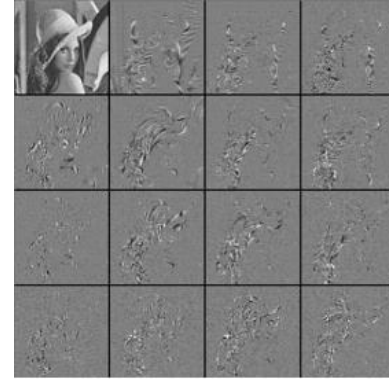


Fig. 7. Two level Wavelet Packet decomposition of image "Lena" using the Daubechies 12 Wavelet family

c) Using the specification extracted from the secret key the Wavelet Packets decomposition of the original image is performed. The multidimensional decomposition is done using successive filter banks. Fig. 7 shows a two level decomposition of the image "Lena" and the levels of detail.

d) The next 16 bits of the secret author's key indicate the size of the binary image used as the mark. The other bits of the key are used to identify the groups of coefficients, where the mark will be embedded. For every bit of the mark a group of N Wavelet Packet coefficients is identified. These groups of coefficients are evenly distributed in the bands of decomposition levels between 2 and $L-1$, where L is the maximum decomposition level of the original image.

e) For every group of coefficients the mean is individually computed. Then the individual quantization levels $q(i,j)$ are obtained (see Equation 1) based on an optimal quantization step Δ . The quantization step is chosen so as to maximize the embedding weight, while minimizing the distortion introduced. Afterwards, each bit of the binary watermark image is inserted in the corresponding group of coefficients by the modification of the individual mean of the group. Rounding the mean to an even quantization level embeds a zero, while rounding the mean to an odd quantization level embeds a one. This is done by rounding the obtained quantization levels $q(i,j)$ to the nearest even / odd quantization levels (to form $q'(i,j)$) and then adjusting the mean of the Wavelet Packets coefficient regions to the computed values (as in Eq. 10 and 11).

$$q(i,j) = \left\lceil \frac{\text{mean}(i,j)}{\Delta} \right\rceil \quad (10)$$

$$\begin{aligned} \text{mark}(n) = 0 &\rightarrow q'(i,j) = \begin{cases} q(i,j) & \text{if } q(i,j) \text{ even} \\ q(i,j) + 1 & \text{if } q(i,j) \text{ odd} \end{cases} \\ \text{mark}(n) = 1 &\rightarrow q'(i,j) = \begin{cases} q(i,j) + 1 & \text{if } q(i,j) \text{ even} \\ q(i,j) & \text{if } q(i,j) \text{ odd} \end{cases} \end{aligned} \quad (11)$$

f) Finally, we apply the appropriate Wavelet Packet synthesis bank on the available coefficients – some modified and some not – to reconstruct the watermarked image. As

shown in Fig. 8, the image produced is visually identical to the original unmarked image.



Fig. 8. Original “Lena” image (left) and watermarked image (right)

At the other end of the communication channel or after the image has been stored, the watermark has to be extracted. The first four steps of the decoding procedure are identical to the embedding ones. The unique, secret key is used to decompose the image in levels of detail according to specific parameters. Then the groups of Wavelet Packets coefficients are selected. The groups of coefficients are examined. First the new mean $\hat{m}\hat{e}\hat{a}\hat{n}(i, j)$ is computed. Then, using the knowledge of the optimal quantization steps, we can calculate the quantization levels and extract the watermarking data (see Eq. 12 and 13).

$$\hat{q}(i, j) = \left\lceil \frac{\hat{m}\hat{e}\hat{a}\hat{n}(i, j)}{\Delta} \right\rceil \quad (12)$$

$$\begin{aligned} \text{mark}(n) &= 0 \text{ if } \hat{q}(i, j) \text{ even} \\ \text{mark}(n) &= 1 \text{ if } \hat{q}(i, j) \text{ odd} \end{aligned} \quad (13)$$

V. EXPERIMENTAL RESULTS

This section describes the experimental results, which verify the capabilities of our watermarking scheme. For this purpose we used real square-size images of resolution greater than 256x256 pixels. We notice that our system is more suitable for photographic-like gray-scale images since they have more detail in which to hide a watermark. The binary images used as watermarks contained a text message and were less than 512 pixels big.

TABLE I
PSNR RESULTS FOR DIFFERENT WAVELET FUNCTIONS

| Wavelet function | Average PSNR [dB] |
|------------------|-------------------|
| Coiflets 12 | 40.23 |
| Coiflets 24 | 39.87 |
| Daubechies 12 | 40.12 |
| Daubechies 16 | 40.28 |
| Bior 4.4 | 41.72 |
| Overall | 40.44 |

First we have made sure that our embedding system does not introduce visual artifacts in images. We have first measured the visual quality of the marked images by qualitative observations. However, to produce more objective results, we have also used the Peak Signal to Noise Ratio

(PSNR). The results obtained for 20 different original images are shown in Table I. We have obtained an average PSNR of 40.44 dB. This is above the usually tolerated degradation level of 40 dB.

The first goal of our project was to develop a watermarking scheme for Copyright protection, that can withstand a certain degree of image compression and resist a series of attacks. Generally speaking, JPEG recommends a quality factor between 75 and 95 for a compressed image to be visually indistinguishable from the original one, and between 50 and 75 to be merely acceptable. Table II and III show the robustness of our Wavelet Packets-based digital watermarking system to high and medium quality JPEG compression and to some attacks as blurring and sharpening.

TABLE II
RESISTENCE OF THE WATERMARKING SCHEME TO JPEG COMPRESSION

| JPEG Quality Factor | 50 | 60 | 70 | 80 | 90 |
|------------------------|-------|-------|-------|-------|-------|
| PSNR after compression | 33.7 | 34.5 | 35.7 | 37.4 | 40.6 |
| Watermark extraction | 96.2% | 97.8% | 98.5% | 99.4% | 99.7% |

TABLE III
RESISTENCE OF THE WATERMARKING SCHEME TO BLURRING, SHARPENING AND MIXED ATTACKS

| Attack type | Blur | Sharpen | Blur+JPEG Comp. with Q=50 | Sharpen+JPEG Comp. with Q=50 |
|------------------------|-------|---------|---------------------------|------------------------------|
| PSNR after attack (dB) | 34.2 | 32.5 | 30.5 | 28.1 |
| Watermark extraction | 95.3% | 98.4% | 92.7% | 94.2% |

REFERENCES

- [1] R. G. van Schyndel, A. Z. Tirkel, and C. F. Osborne, “A digital watermark,” in *IEEE Proceedings ICIP*, vol.2, pp. 86-90, 1994.
- [2] N. Nikolaidis, and I. Pitas, “Copyright protection of images using robust digital signatures,” in *IEEE Int. Conf. Acoustics, Speech Signal Processing*, vol. 4, pp.2168-2171, May1996.
- [3] R. Wolfgang and E. Delp, “A watermark for digital image,” in *IEEE ICIP*, vol.3, pp.211-214, 1996.
- [4] M.-S. Hsieh, D.-C. Tseng, and Y.-H. Huang, “Hiding Digital Watermarks Using Multiresolution Wavelet Transform,” in *IEEE. Trans. Industrial Electronics*, vol. 48, no. 5, pp. 875-882, 10/2001
- [5] H. Daren, L. Jiufen, H. Jiwu, and L. Hongmei, “A DWT-based image watermarking algorithm,” in *Proceedings IEEE Int. Conf. Multimedia and Expo*, Tokyo, 22-25/8/2001.
- [6] R.R. Coifman and Y. Meyer, “Orthonormal wave packet bases”, in Technical report, Dept. of Mathematics, Yale University, 1990.
- [7] D.N. Vizireanu, C. Pirnog, “*Nonlinear Digital Signal Processing*”, “Electronica 2000”, Bucharest, 2001, Romania.
- [8] D.N. Vizireanu, C. Pirnog, A. Vizireanu - “The Skeleton Structure - An Improved Compression Algorithm with Perfect Reconstruction”, *Journal of Digital Imaging*, VOL. 14, NO. 2, June 2001, Orlando, Florida, USA, p. 241-242.